

vGamba: Attentive State Space Bottleneck for efficient Long-range Dependencies in Visual Recognition

Yunusa Haruna
Beihang University and NewraLab

Adamu Lawan
Beihang University

Abstract

Capturing long-range dependencies efficiently is essential for visual recognition tasks, yet existing methods face limitations. Convolutional neural networks (CNNs) struggle with restricted receptive fields, while Vision Transformers (ViTs) achieve global context and long-range modeling at a high computational cost. State-space models (SSMs) offer an alternative, but their application in vision remains underexplored. This work introduces vGamba, a hybrid vision backbone that integrates SSMs with attention mechanisms to enhance efficiency and expressiveness. At its core, the Gamba bottleneck block that includes, Gamba Cell, an adaptation of Mamba for 2D spatial structures, alongside a Multi-Head Self-Attention (MHSA) mechanism and a Gated Fusion Module for effective feature representation. The interplay of these components ensures that vGamba leverages the low computational demands of SSMs while maintaining the accuracy of attention mechanisms for modeling long-range dependencies in vision tasks. Additionally, the Fusion module enables seamless interaction between these components. Extensive experiments on classification, detection, and segmentation tasks demonstrate that vGamba achieves a superior trade-off between accuracy and computational efficiency, outperforming several existing models.

1. Introduction

Modeling long-range dependencies is essential in visual recognition for interpreting complex scenes where objects of interest span large spatial regions, such as in instance segmentation or aerial imagery. Traditional convolutional neural networks (CNN) backbones have dominated the field [4, 13, 27, 32, 33], and while their hierarchical structure allows effective feature extraction, their strong inductive bias and local receptive fields limit their ability to model long-range dependencies. To mitigate this limitation, techniques such as dilated convolutions have been used to expand the receptive field [41, 42], and non-local neural net-

works have shown promise in capturing long-range dependencies [35]. However, these approaches often struggle to efficiently model long-range dependencies and global context, which is essential to understanding intricate relationships in visual recognition. Consequently, Vision Transformers (ViT) [7] have gained popularity for their ability to capture long-range dependencies using self-attention mechanisms, which allow them to model global context more effectively than CNN. However, the computational complexity of self-attention scales quadratically with sequence length, making ViT computationally expensive, especially for high-resolution images and real-time applications. Various techniques, such as low-rank factorization [40], linear approximation [23, 30], and sparse attention [3], have been proposed to reduce computational costs while preserving performance. However, these approaches often involve trade-offs between efficiency and effectiveness.

State-space models (SSM) [11] have recently emerged as an alternative to attention mechanisms, offering a more efficient way to model long-range dependencies. By capturing sequential dependencies in a compact form, SSMs reduce computational overhead while maintaining competitive performance. Mamba [10], a selective state space model, was introduced to further optimize efficiency, achieving 5x higher throughput than transformers by selectively retaining relevant information and removing redundant details. Although Mamba has shown success in tasks such as time series prediction, its application to image-based tasks remains limited, and its performance has to match that of attention-based models in complex vision tasks. Despite this, research on adapting SSM to vision tasks, such as ViM [45] and VMamba [19], remains relatively unexplored.

Given the strengths and weaknesses of both ViT and SSM, hybrid models that combine attention mechanisms with state-space modeling present a promising research direction [12]. Although many hybrid approaches have been explored in NLP, such as MambaForGCN [15], Samba [28], Jamba [17], and Zamba [9], as well as in time series analysis, including SST [38], SiMBA [25], FMamba [22], and Bi-mamba [16], their application in computer vision re-

mains underexplored. The potential of hybrid backbones lies in their ability to leverage the efficiency of SSM while maintaining the expressiveness of attention mechanisms.

To this end, we propose vGamba, a hybrid vision backbone model designed to efficiently capture long-range dependencies in visual recognition. At its core, vGamba is built upon the Gamba Block, a bottleneck structure inspired by CNN bottlenecks, making it compatible with architectures like ResNet [13]. The Gamba Block consists of three key components. First, the Gamba Cell extends Mamba for vision tasks by adapting it to handle 2D spatial structures. It also incorporates positional embeddings and spatial context awareness to enhance feature representation. The second component, the Multi-Head Self-Attention (MHSA) mechanism, is specifically adapted for vision tasks and utilizes 2D positional embeddings and register tokens to improve spatial encoding and global context modeling. Lastly, a Gated Fusion Module, which seamlessly integrates the outputs from both the Gamba Cell and the MHSA Module, facilitating efficient interaction between them to ensure optimal feature fusion. By combining these components, Gamba Block enables vGamba to enhance representational efficiency and contextual understanding, making it a powerful alternative to traditional vision backbones.

The contributions of this work are summarized below:

- We propose vGamba, a hybrid vision backbone model designed to efficiently capture global context and long-range dependencies in complex images through an attentive state-space approach.
- We introduce Gamba Block, a novel bottleneck structure that combines a global 2D state-space modeling with attention mechanisms, designed for vision tasks, and the Gamba Cell, a key component that extends the Mamba model to vision, incorporating spatial context and positional embeddings for enhanced feature representation.
- Experimental results on classification, detection, and object segmentation tasks demonstrate that vGamba outperforms several existing models, due to its enhancements in capturing global context and long-range dependencies.

2. Related Work

CNN is highly effective for many vision tasks, but they struggle to capture long-range dependencies due to their small, localized filters. As layers deepen, the receptive field increases but remains limited within a fixed structure, making it difficult to model distant relationships. To address this, approaches such as dilated convolutions have been introduced to expand the receptive field without sacrificing resolution. For example, Yu et al. (2017) [42] proposed Dilated Residual Network (DRN), replacing subsampling layers with dilated convolutions, maintaining high-resolution feature maps while improving object localization and semantic segmentation tasks. Similarly, [41] (2016) [41] in-

roduced a multi-scale context aggregation module for semantic segmentation that uses dilated convolutions to capture multi-scale context while preserving resolution. In contrast, Non-Local Neural Networks [35] address long-range dependencies by computing the response of a position as a weighted sum of features of all positions in the input, efficiently handling spatial and temporal dependencies in images, videos, and sequences. Although these methods mitigate the challenges of modeling long-range dependencies, they still fail to capture global context with the same level of efficiency as attention mechanisms. Specifically, dilated convolutions can suffer from gridding effects and limited global coverage, while non-local networks introduce redundancy and are computationally expensive.

ViT overcome the limitations of CNNs in modeling long-range dependencies and global context from the first layer by treating image patches as tokens and computing relationships between all patches using attention mechanisms, allowing the direct capture of long-range dependencies. Although ViT has shown compelling performance in image classification, segmentation, and detection [7], they require large datasets for effective training and are computationally expensive due to dense self-attention. This leads to significant challenges, especially the quadratic time complexity in both self-attention (SA) and backpropagation. To address these limitations, techniques like low-rank approximations have been proposed. For example, Yang et al. (2024) [40] introduced Low-rank BackPropagation via Walsh-Hadamard Transformation, which reduces backpropagation costs by projecting gradients into a low-rank space, maintaining efficiency without sacrificing accuracy. Another approach is to use a linear approximation. Ma et al. (2021) [23] introduced linear attention mechanisms, termed Luna, to approximate traditional attention with two nested linear functions, reducing the complexity of time and memory from quadratic to linear. Similarly, Song (2021) [30] proposed UFO-ViT, which replaces softmax with L2-norm in SA, resulting in linear complexity while maintaining competitive performance in image classification and dense prediction. In contrast, Chen et al. (2023) [3] proposed SparseViT, which applies window-level activation pruning, reducing latency by 50% with 60% sparsity and achieving significant speedup in high-resolution tasks with minimal accuracy loss. While these methods excel at modeling long-range dependencies and global context, they are still computationally and memory-constrained.

Gu and Dao (2023) proposed Mamba [10], which addresses the high computational and memory costs of attention mechanisms using a discretized state-space model (SSM). By adapting continuous SSM mechanisms for deep learning tasks, it provides a more efficient alternative while achieving compelling results in autoregressive tasks [1, 28, 29, 39], though not inherently optimized for vision applica-

tions. To address this, various modifications have been proposed, such as VMamba [19] that adapt the original Mamba architecture by replacing its causal structure with cross-scan to improve the capture of long-range dependencies in images. In contrast, ViM [45] used positional embeddings to mark input sequences, then used a bidirectional SSM to compress the visual representation. These adaptation results are promising, making Mamba as an efficient alternative to ViTs, particularly for handling large-scale and complex image data.

The integration of Mamba with attention mechanisms for visual tasks remains largely unexplored. The synergy between ViT and SSM in vision tasks has received limited attention. Given their complementary strengths, efficiency in Mamba and accuracy in ViT hybrid ViT-SSM models could provide significant advantages in efficiently modeling long-range dependencies. However, their application in computer vision has yet to be fully investigated.

This gap in the current literature motivates our work, in which we combine the Mamba SSM approach with self-attention mechanisms, adapting it to conventional vision models. Using Mamba efficiency and attention model accuracy, we can achieve the best of both worlds.

3. Preliminaries

3.1. SSM

SSM represents an input sequence $x(t) \in \mathbb{R}$ through a latent state $h(t) \in \mathbb{R}^N$ using the following continuous linear system:

$$\begin{aligned} h'(t) &= Ah(t) + Bx(t), \\ y(t) &= Ch(t) + Dx(t) \end{aligned} \quad (1)$$

where $A \in \mathbb{R}^{N \times N}$ is the state transition matrix, $B \in \mathbb{R}^{N \times 1}$ maps the input to the state, $C \in \mathbb{R}^{1 \times N}$ maps the state to the output, and $D \in \mathbb{R}$ is a feedthrough term.

To apply SSMs in deep learning, the continuous system is discretized using the zero-order hold (ZOH) method, which assumes the input remains constant over each time step Δt . The discretized system is:

$$\hat{A} = e^{A\Delta t}, \quad \hat{B} = \left(\int_0^{\Delta t} e^{A\tau} d\tau \right) B \quad (2)$$

This leads to the discrete recurrence:

$$\begin{aligned} h_k &= \hat{A}h_{k-1} + \hat{B}x_k, \\ y_k &= Ch_k + Dx_k \end{aligned} \quad (3)$$

Traditional SSMs use fixed parameters (A, B, C, D) , which limits their ability to adapt to complex, high-dimensional data such as images. Mamba addresses this limitation by making B, C , and the discretization scale input-dependent.

This allows the model to dynamically adjust feature representations, selectively retain relevant information, and efficiently model long-range dependencies.

3.2. Attention Mechanism

The attention mechanism, initially introduced in NLP, has become a key component in various tasks, including computer vision. It allows a model to focus on different parts of the input data when generating an output, improving the representation of long-range dependencies and context.

In its simplest form, the attention mechanism computes a weighted sum of input features, where the weights (or attention scores) are determined by a similarity measure between a query and a set of keys. The mechanism is defined eqn (4):

$$\text{Attention}(Q, K, V) = \text{softmax} \left(\frac{QK^T}{\sqrt{d_k}} \right) V \quad (4)$$

Here, $Q \in \mathbb{R}^{n_q \times d_k}$ represents the query matrix, $K \in \mathbb{R}^{n_k \times d_k}$ represents the key matrix, and $V \in \mathbb{R}^{n_k \times d_v}$ represents the value matrix. The term d_k is the dimensionality of the key vectors. The softmax function is applied to the similarity between the query and the keys, normalizing the weights and allowing the model to focus on the most relevant parts of the input.

4. Method

This section discusses the design method of Gamba Bottleneck Block, which includes, Gamba Cell, 2D MHSA, Fusion Mechanism, and its architectural details. Fig. (1) illustrates in details these components.

4.1. Gamba Cell

The original Mamba model utilizes causality, which is effective for autoregressive tasks but suboptimal for vision applications, where all pixels are processed simultaneously without prior token dependency. In autoregressive settings, each token depends strictly on the preceding ones, ensuring sequential consistency. However, in vision tasks, this causal constraint introduces long-range decay, where dependencies weaken over distance, leading to reduced effectiveness. As shown in eqn (3), the i -th token in the original Mamba model depends only on the $(i - 1)$ -th token, forming a chain-like structure. This sequential dependency is inefficient for vision, where spatial relationships vary across the image. To overcome this, the Mamba Cell removes the strict causality, allowing pixels to interact flexibly across the entire context, thereby enhancing long-range interactions and improving performance. However, removing causality alone is not enough—efficiently capturing spatial dependencies remains crucial. To address this, we introduce a 2D positional encoding that encodes both horizontal and vertical relationships, ensuring that spatial interactions are preserved without relying on causal constraints. Additionally,

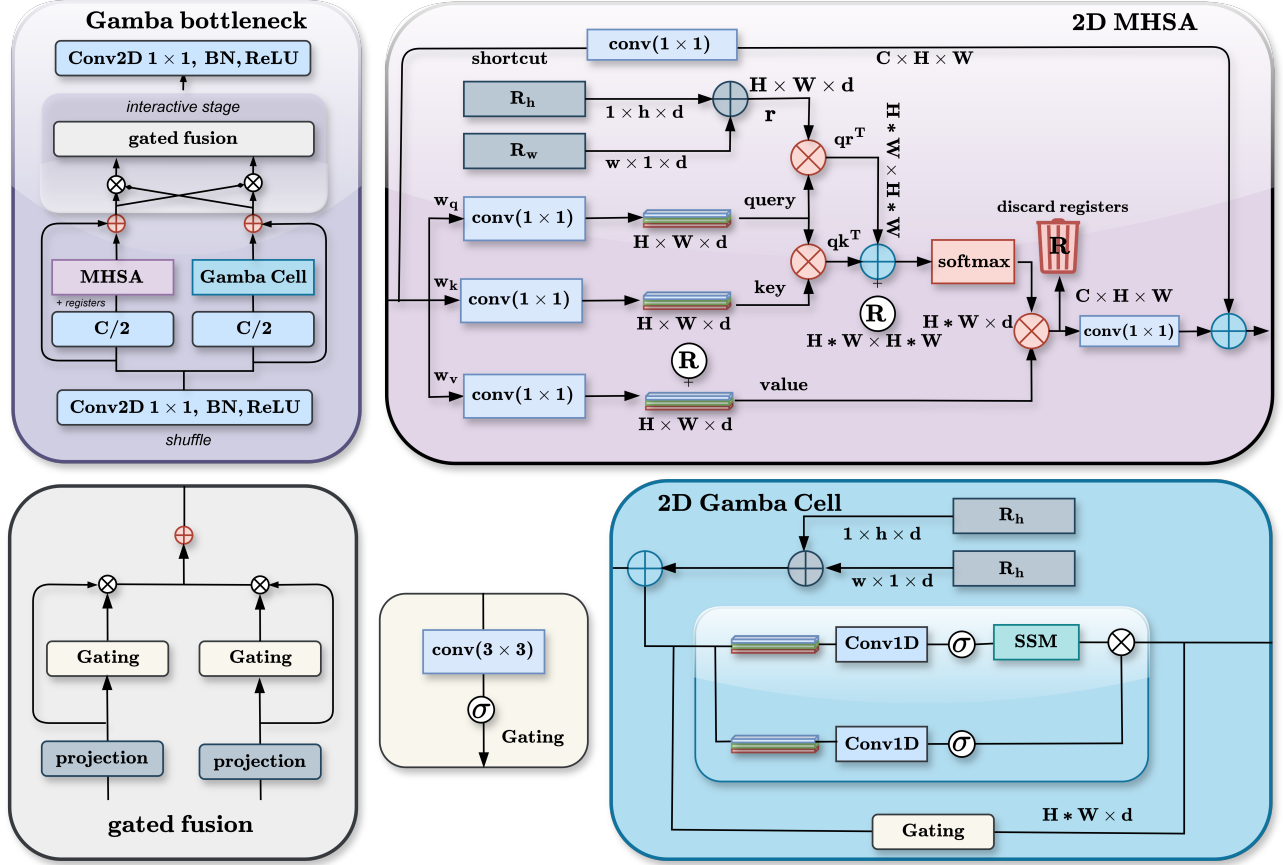


Figure 1. Gamba Bottleneck showing Gamba Cell, 2D MHSA and it's gating fusion.

we incorporate a spatial context-aware mask, which effectively modulates feature interactions while preserving computational efficiency. This combined approach ensures that spatial dependencies are captured without excessive complexity, making our method more practical for vision applications. Given an input feature tensor.

$$X \in \mathbb{R}^{B \times C \times H \times W}, \quad (4)$$

where B is the batch size, C the number of channels, and H, W the spatial dimensions, we first reshape it into a sequence representation:

$$X \rightarrow X_{\text{seq}} \in \mathbb{R}^{B \times (HW) \times C}, \quad (5)$$

To encode spatial priors, we introduce learnable relative positional embeddings along the height and width dimensions:

$$P = R_h + R_w, \quad P \in \mathbb{R}^{1 \times C \times (HW)}, \quad (6)$$

where R_h and R_w are trainable parameters capturing positional biases. The input is then enriched with positional information:

$$X_{\text{seq}} = X_{\text{seq}} + P^T, \quad (7)$$

A spatial context-aware mask is then applied using a 1D convolution followed by a sigmoid activation, generating a context-aware gating mechanism:

$$G = \sigma(\text{Conv1D}(X_{\text{seq}}^T)), \quad (8)$$

where σ denotes the sigmoid function. Simultaneously, the sequence is processed through a Mamba block, denoted as M , which captures long-range dependencies:

$$X_{\text{mamba}} = M(X_{\text{seq}}), \quad (9)$$

Then the output is computed as an element-wise interaction between gated context and the Mamba-enhanced features:

$$X_{\text{out}} = X_{\text{mamba}} \odot G, \quad (10)$$

where \odot denotes element-wise multiplication. The final representation is reshaped back to the spatial domain:

$$X_{\text{out}} \in \mathbb{R}^{B \times C \times H \times W}, \quad (11)$$

This approach eliminates causality constraints, making the model better suited for vision tasks by enabling global spatial interactions while maintaining efficiency. The use of a

spatial context-aware mask ensures that dependencies are captured adaptively, avoiding the computational burden introduced by bidirectional [45] or cross-scan strategies [19].

4.2. 2D-MHSA

To enhance vGamba performance, we integrate a global 2D-MHSA, following [43]. While Mamba efficiently captures long-range dependencies with 5× lower computational complexity, self-attention achieves superior performance. By incorporating 2D-MHSA, our model effectively balances long-range and global context processing, enhancing spatial relationship modeling.

Given a 2D feature map $F \in \mathbb{R}^{H \times W \times C}$, we reshape it into a sequence and compute queries Q , keys K , and values V using learned weight matrices. Attention scores are derived via the dot product of Q and K , followed by softmax normalization. The output is computed as a weighted sum of V , capturing full-image dependencies rather than just local ones. To preserve spatial coherence, we employ a 2D relative positional encoding, ensuring that attention mechanisms focus on relevant regions based on their relative spatial positions [31]. This approach effectively balances long-range and global interactions, improving contextual understanding while maintaining computational efficiency.

4.3. Interaction and Fusion Mechanism

The fusion of 2D-Mamba and 2D-MHSA is critical for leveraging the best of both worlds. While 2D-Mamba efficiently captures long-range patterns with reduced computational cost, 2D-MHSA excels in modeling global relationships but is more expensive. A structured fusion mechanism is necessary to leverage their complementary strengths. To achieve this, we employ a gating-based fusion strategy. The model first splits the feature map along the channel dimension, processing one half with 2D-Mamba and the other with 2D-MHSA. Their outputs are then adaptively fused using a gating mechanism that learns to balance long and global representations. Specifically, learned conv-based projections transform each output, and sigmoid-activated gating weights determine their contributions.

Given two outputs x_{mamba} and x_{mhSA} , fusion is computed:

$$\begin{aligned} \text{Gate}_m &= \sigma(W_m * x_{\text{mamba}}), \\ \text{Gate}_h &= \sigma(W_h * x_{\text{mhSA}}) \end{aligned} \quad (12)$$

$$x_{\text{fused}} = \text{Gate}_m \cdot W_m * x_{\text{mamba}} + \text{Gate}_h \cdot W_h * x_{\text{mhSA}} \quad (13)$$

where W_m and W_h are learnable projections, and $\sigma(\cdot)$ is the sigmoid function. This ensures that the network dynamically adjusts the contribution of each block based on the input context.

This fusion mechanism enhances the model’s ability to capture spatial patterns while maintaining computational efficiency, leading to improved feature representation and overall performance.

4.4. Architectural details

The first two stages capture local details and perform low-level feature extraction, where the input $x \in \mathbb{R}^{C \times H \times W}$ is processed through a stem layer and standard ResNet bottleneck blocks [13]. These layers extract hierarchical features while progressively reducing spatial dimensions:

$$x_1 \in \mathbb{R}^{C_1 \times \frac{H}{4} \times \frac{W}{4}}, \quad x_2 \in \mathbb{R}^{C_2 \times \frac{H}{8} \times \frac{W}{8}}$$

For Stages 3 and 4, we replace the ResNet blocks with Gamba bottleneck blocks, enhancing long-range dependencies and global context modeling. The hybrid vGamba captures feature representations at deeper levels:

$$x_3 \in \mathbb{R}^{C_3 \times \frac{H}{16} \times \frac{W}{16}}, \quad x_4 \in \mathbb{R}^{C_4 \times \frac{H}{32} \times \frac{W}{32}}$$

Finally, global average pooling (GAP) and a fully connected layer (FC) produce the final classification output:

$$y = \text{FC}(\text{GAP}(x_4))$$

4.4.1. Variants

Model	GFLOP	Param	Depth	Blocks
vGamba-B	3.77G	18.94M	50	[3, 4, 6, 3]
vGamba-L	6.32G	31.89M	101	[3, 4, 23, 3]

Table 1. Variants of vGamba-Baseline and vGamba-Large

5. Experiments

We evaluated vGamba on ImageNet-1K for classification (Section 5.1), ADE20K for segmentation (Section 5.2), and COCO for detection (Section 5.3). Additionally, we conducted experiments on the AID dataset (Section 5.4) and performed ablation studies (Section 5.5).

5.1. Classification

Settings. The ImageNet-1K dataset [6] contains 1.28M training images and 50K validation images across 1,000 categories. Training follows ConvNeXt [21] settings, using augmentations like random cropping, flipping, label-smoothing, mixup, and random erasing. For 224^2 input images, we optimize with AdamW with momentum 0.9, batch size 64, and weight decay 0.05. Then trained vGamba models for 250 epochs with a cosine schedule and EMA, starting with a 1×10^{-3} learning rate. Testing includes center cropping to 224^2 images. Experiments are conducted on 8 NVIDIA Titan XP 12GB GPUs.

Results. Table (2) vGamba, achieves better performance in efficiency and accuracy compared to CNNs, Transformers, and existing SSMs. vGamba-L attains the highest Top-1

Table 2. Model performance comparison on ImageNet-1K.

Method	IMAGENET-1K				
	Size	FLOPs	Param	TP	Top-1
	(G)	(M)	(img/s)	(%)	
ResNet-50 [13]	224 ²	3.9G	25M	1226.1	76.2%
ResNet-101 [13]	224 ²	7.6G	45M	753.6	77.4%
ResNet-152 [13]	224 ²	11.3G	60M	526.4	78.3%
BoT50 [31]	224 ²	-	20.8M	-	78.3%
EffNet-B2 [33]	224 ²	1.0G	9M	1255.7	80.1%
EffNet-B3 [33]	300 ²	1.8G	12M	732.1	81.6%
RegNetY-4GF [27]	224 ²	4.0G	21M	1156.7	80.0%
RegNetY-8GF [27]	224 ²	8.0G	39M	591.6	81.7%
ViT-B/16 [7]	384 ²	55.4G	86M	85.9	77.9%
ViT-L/16 [7]	384 ²	190.7G	307M	27.3	76.5%
DeiT-S [34]	224 ²	4.6G	22M	940.4	79.8%
DeiT-B [34]	224 ²	17.5G	86M	292.3	81.8%
Swin-T [20]	224 ²	4.5G	29M	755.2	81.3%
CoaT-Lite-S [5]	224 ²	4.1G	19.8M	2269	82.3%
CrossViT-B [2]	240 ²	20.1G	105.0M	1321	82.2%
Vim-S [45]	224 ²	5.3G	26M	811	80.3%
Vim-B [45]	224 ²	-	98M	-	81.9%
EffVMamba-T [26]	224 ²	0.8G	6M	2904	76.5%
EffVMamba-S [26]	224 ²	1.3G	11M	1610	78.7%
S4ND-ViT-B [24]	224 ²	17.1G	89M	397	80.4%
VMamba-T [19]	224 ²	4.9G	30M	1686	82.6%
MambaVision-T [12]	224 ²	4.4G	31.8M	6298	82.3%
vGamba-B	224 ²	3.77G	18.94M	1125	81.1%
vGamba-L	224 ²	6.32G	31.89M	746.2	82.8%

accuracy (82.8%) while maintaining a lower computational cost (6.32G FLOPs, 31.89M parameters) compared to ViTs and other SSMs. Compared to ViT-B/16, which requires 55.4G FLOPs and 86M parameters for a Top-1 accuracy of 77.9%, vGamba-L is significantly more efficient while outperforming it by 4.9%. Additionally, vGamba-L outperforms MambaVision-T (82.3%) and VMamba-T (82.6%). vGamba demonstrates an optimal balance of accuracy, efficiency, and scalability, making it a promising architecture for real-world applications requiring high-performance vision models.

5.2. Segmentation

Settings. We conducted semantic segmentation experiments using the ADE20K dataset [44] within the UperNet framework [37]. The backbone network was initialized with pre-trained weights from ImageNet-1K [6], while the remaining components were randomly initialized. Model optimization was performed using the AdamW optimizer with a batch size of 16. The model was trained for 160k iterations to ensure thorough learning.

Table 3. Comparison of semantic segmentation results on ADE20K using UperNet. FLOPs are measured with an input size of 512×2048.

Backbone	ADE20K			
	Param	FLOP	mIoU	mIoU
	(M)	(G)	(SS)	(MS)
ResNet-50 [13]	67	953	42.1	42.8
ResNet-101 [13]	85	1030	42.9	44.0
ConvNeXt-T [21]	60	939	46.0	46.7
ConvNeXt-S [21]	82	1027	48.7	49.6
DeiT-S + MLN [34]	58	1217	43.8	45.1
DeiT-B + MLN [34]	144	2007	45.5	47.2
Swin-T [20]	60	945	44.5	45.8
Swin-S [20]	81	1039	47.6	49.5
Swin-B [20]	121	1188	48.1	-
Vim-S [45]	46	-	44.9	-
VMamba-T [19]	62	949	47.9	48.8
VMamba-S [19]	82	1028	50.6	51.2
VMamba-B [19]	122	1170	51.0	51.6
EfficientVMamba-T [26]	14	230	38.9	39.3
EfficientVMamba-S [26]	29	505	41.5	42.1
EfficientVMamba-B [26]	65	930	46.5	47.3
vGamba-B	55	941	50.9	51.3
vGamba-L	71	1019	51.4	52.2

Results. Table (3), vGamba achieves state-of-the-art performance in semantic segmentation on ADE20K, outperforming both CNNs and Transformer-based models while maintaining computational efficiency. Its ability to effectively model long-range dependencies and spatial coherence enables better segmentation accuracy with lower computational overhead compared to ViT. vGamba-L achieves the highest mIoU of 51.4 (SS) and 52.2 (MS), surpassing vGamba-B (50.9, 51.3) and Swin-B (48.1, -). Similarly, vGamba-B maintains good performance at 50.9 (SS) and 51.3 (MS) with fewer parameters than larger ViTs. These results establish vGamba as a highly effective alternative for semantic segmentation, offering a balance of accuracy and efficiency that makes it good for real-world applications.

5.3. Object Detection

Settings. We evaluated our model on object detection and instance segmentation tasks using the COCO 2017 dataset [18], which consists of approximately 118K training images and 5K validation images. vGamba was utilized as the backbone and integrated into the Mask R-CNN framework [14] for feature extraction. The model was initialized with weights pre-trained on ImageNet-1K (300 epochs) and trained for 12 epochs (1×) and 36 epochs (3×).

Results Table (4) The comparison of vGamba with other

models in Mask R-CNN and Cascade Mask R-CNN detection tasks reveals notable performance.

- In the Mask R-CNN 1× schedule, vGamba-B achieves an AP_b of 44.9 and AP_m of 42.0, with lower FLOPs (225G) and fewer parameters (49M) compared to other models. The larger vGamba-L improves to 49.8 and 45.3 for AP_b and AP_m , respectively, while having good computational requirements.
- In the Mask R-CNN 3× MS schedule, vGamba-L demonstrates impressive performance with AP_b at 51.3 and AP_m at 46.1, surpassing several larger models like Swin-S and ConvNeXt-S in terms of both accuracy and efficiency.
- For Cascade Mask R-CNN 3× MS schedule, vGamba-B outperforms models like Swin-T and ConvNeXt-T with an AP_b of 50.8 and AP_m of 43.7. The larger vGamba-L performs similarly to the top-performing models, achieving 53.1 for AP_b and 46.3 for AP_m , with fewer computational resources than some alternatives.

These results indicate that vGamba provides competitive performance, offering high accuracy while maintaining efficiency in terms of computational cost.

5.4. Additional Experiments

We performed qualitative experiments using Hi-Res Grad-CAM [8] on the AID aerial dataset [36] due to its inherent long-range dependencies to analyze the model’s decision-making. The visualized attention highlights both local features and broader context, such as runway layouts and surrounding infrastructure, demonstrating the model’s ability to capture long-range dependencies in complex aerial scenes. These results confirm the model’s effectiveness and explainability for aerial scene understanding Fig (2).

5.5. Ablation

5.5.1. Effects of components

We determine the contribution of each component in vGamba. We removed each components and analyze their effects on accuracy and efficiency.

Results. we observed that adding the Fusion component improves accuracy to 81.1 while maintaining efficiency (similar FLOP and parameter count). Also, the combination of Gamba Cell + MHSA also improves accuracy to 79.3 while slightly reducing FLOP compared to Gamba Cell alone.

Table 6 evaluates the impact of removing key components from Gamba Cell on classification performance, with a baseline Top-1 accuracy of 77.9%. Removing the spatial context-aware mask leads to a 1.1% drop (76.8%), indicating it effect that enhance feature interactions and accuracy. In contrast, removing positional embeddings results in a more significant decline to 73.9% (4.0% drop), highlighting its critical role in maintaining spatial coherence and guiding feature learning. These findings suggest that both spatial

Table 4. Cascade Mask R-CNN detection results.

Backbone	FLOPs (G)	Params (M)	AP_b	AP_m
Mask R-CNN 1× schedule				
Swin-T [20]	267G	48M	42.7	39.3
ConvNeXt-T [21]	262G	48	44.2	40.1
VMamba-T [19]	271G	50	47.3	42.7
Swin-S [20]	354G	69	44.8	40.9
ConvNeXt-S [21]	348G	70	45.4	41.8
VMamba-S [19]	349G	70	48.7	43.7
Swin-B [20]	496G	107	46.9	42.3
ConvNeXt-B [21]	486G	108	47.0	42.7
VMamba-B [19]	485G	108	49.2	44.1
vGamba-B	225G	49	44.9	42.0
vGamba-L	254G	71	49.8	45.3
Mask R-CNN 3× MS schedule				
Swin-T [20]	267G	48	46.0	41.6
ConvNeXt-T [21]	262G	48	46.2	41.7
VMamba-T [19]	271G	50	48.8	43.7
Swin-S [20]	354G	69	48.2	43.2
ConvNeXt-S [21]	348G	70	47.9	42.9
VMamba-S [19]	349G	70	49.9	44.2
vGamba-L	254G	71	51.3	46.1
Cascade Mask R-CNN 3× MS schedule				
DeiT-Small/16 [34]	889G	80	48.0	41.4
ResNet-50 [13]	739G	82	46.3	40.1
Swin-T [20]	745G	86	50.4	43.7
ConvNeXt-T [21]	741G	86	50.4	43.7
MambaVision-T [12]	740G	86	51.0	44.3
Swin-S [20]	838G	107	51.9	45.0
ConvNeXt-S [21]	827G	108	51.9	45.0
MambaVision-S [12]	828G	108	52.1	45.2
Swin-B [20]	982G	145	51.9	45.0
ConvNeXt-B [21]	964G	146	52.7	45.6
MambaVision-B [12]	964G	145	52.8	45.7
vGamba-B	727G	76	50.8	43.7
vGamba-L	905G	123	53.1	46.3

Table 5. Gamba bottleneck analysis

Model (components)	Size	Top-1	FLOP	Param
MHSA	224 ²	78.9	3.68G	18.94M
vGambaCell	224 ²	77.9	4.24G	21.81M
vGambaCell + MHSA	224 ²	79.3	3.73G	18.92M
vGambaCell + MHSA + Fusion	224 ²	81.1	3.77G	18.94M

adaptation and positional encoding contribute to improved performance, with positional embeddings having more impact.

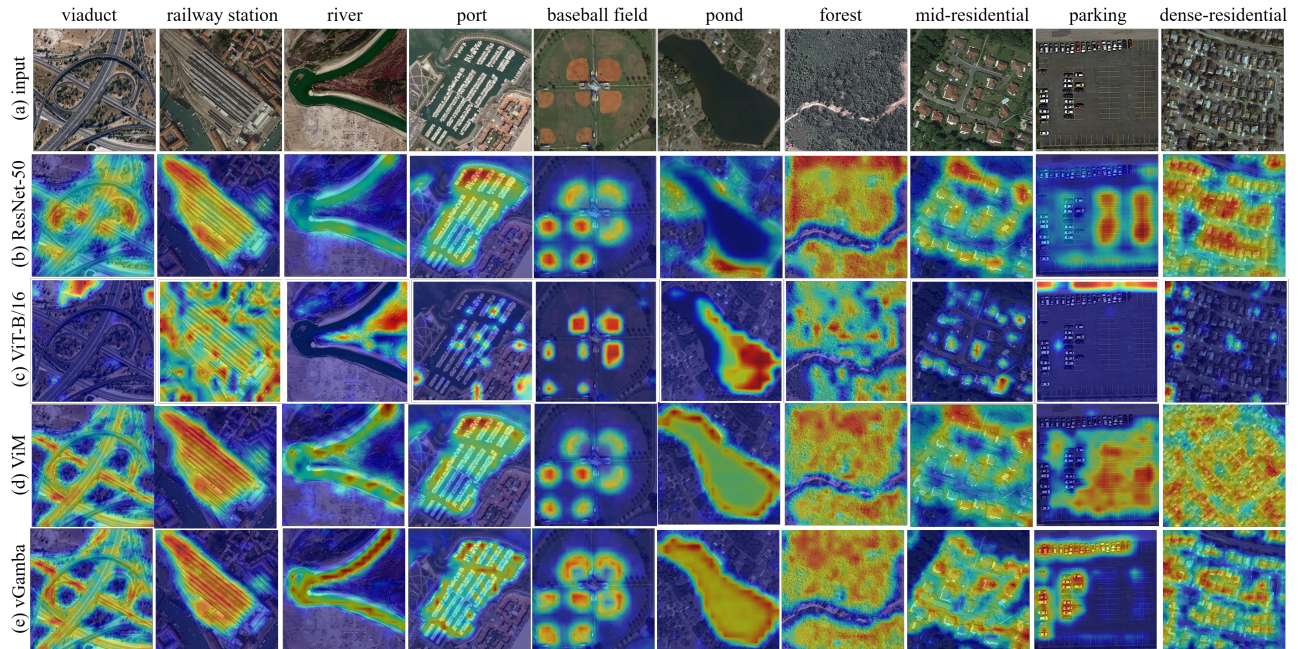


Figure 2. Hi-Res CAM visualization on the Aerial Image dataset, highlighting model decision regions through heatmaps

Table 6. Gamba Cell

Settings	Top-1
Removing the spatial context-aware mask	76.8
Removing the positional embeddings	73.9

6. Conclusion

vGamba offers an efficient hybrid approach for modeling long-range dependencies in visual recognition tasks by combining state-space models with attention mechanisms. The model utilizes the Gamba bottleneck Block, which integrates the Gamba Cell, Multi-Head Self-Attention (MHSA), and a Gated Fusion Module to enhance feature representation and maintain computational efficiency. Through extensive experiments, vGamba demonstrates superior performance in classification, detection, and segmentation tasks, effectively capturing global context and long-range dependencies while outperforming existing models. This work highlights the potential of hybrid SSM-attention models for advancing computer vision applications.

6.1. Limitations

Despite the promising results, there are some limitations in this work. First, while vGamba effectively models long-range dependencies, it is still sensitive to the choice of hyperparameters, particularly in the fusion of the attention and state-space components. Tuning these parameters for differ-

ent vision tasks may require additional experimentation and could lead to variations in performance.

Second, while the integration of 2D-MHSA enhances global context modeling, it introduces additional computational overhead compared to traditional convolutional methods, especially for real-time applications or large-scale datasets. Finally, while vGamba outperforms existing models in benchmark tasks, its performance in highly complex or domain-specific applications, such as those requiring extreme precision (e.g., medical imaging), remains unexplored. Future work will need to address these challenges, including optimizing computational efficiency and extending the model to handle more complex scenarios.

6.2. Broader Impact

vGamba model, with its efficient capture of long-range dependencies, has broad applications across healthcare (e.g., medical image analysis for tumor detection), autonomous driving (enhancing object detection in complex environments), robotics (improving visual perception for navigation and manipulation), and aerial vision (optimizing analysis of surveillance and environmental monitoring). Its ability to process high-resolution images efficiently makes vGamba a valuable tool for real-time vision systems across diverse industries.

References

- [1] Raunaq Bhirangi, Chenyu Wang, Venkatesh Pattabiraman, Carmel Majidi, Abhinav Gupta, Tess Hellebrekers, and Lerrel Pinto. Hierarchical state space models for continuous sequence-to-sequence modeling. *arXiv preprint arXiv:2402.10211*, 2024. 2
- [2] Chun-Fu Richard Chen, Quanfu Fan, and Rameswar Panda. Crossvit: Cross-attention multi-scale vision transformer for image classification. In *Proceedings of the IEEE/CVF International Conference on Computer Vision*, pages 357–366, 2021. 6
- [3] Xuanyao Chen, Zhijian Liu, Haotian Tang, Li Yi, Hang Zhao, and Song Han. Sparsevit: Revisiting activation sparsity for efficient high-resolution vision transformer. In *Proceedings of the IEEE/CVF Conference on Computer Vision and Pattern Recognition*, pages 2061–2070, 2023. 1, 2
- [4] François Chollet. Xception: Deep learning with depthwise separable convolutions. In *Proceedings of the IEEE conference on computer vision and pattern recognition*, pages 1251–1258, 2017. 1
- [5] Zihang Dai, Hanxiao Liu, Quoc V. Le, and Mingxing Tan. Coatnet: Marrying convolution and attention for all data sizes. In *Advances in Neural Information Processing Systems*, pages 3965–3977, 2021. 6
- [6] Jia Deng, Wei Dong, Richard Socher, Li-Jia Li, Kai Li, and Li Fei-Fei. Imagenet: A large-scale hierarchical image database. In *2009 IEEE conference on computer vision and pattern recognition*, pages 248–255. Ieee, 2009. 5, 6
- [7] Alexey Dosovitskiy, Lucas Beyer, Alexander Kolesnikov, Dirk Weissenborn, Xiaohua Zhai, Thomas Unterthiner, Mostafa Dehghani, Matthias Minderer, Georg Heigold, Sylvain Gelly, Jakob Uszkoreit, and Neil Houlsby. An image is worth 16x16 words: Transformers for image recognition at scale. In *ICLR*, 2021. 1, 2, 6
- [8] Rachel Lea Draelos and Lawrence Carin. Use hirescam instead of grad-cam for faithful explanations of convolutional neural networks. *arXiv preprint arXiv:2011.08891*, 2020. 7
- [9] Paolo Glorioso, Quentin Anthony, Yury Tokpanov, James Whittington, Jonathan Pilault, Adam Ibrahim, and Beren Millidge. Zamba: A compact 7b ssm hybrid model. *arXiv preprint arXiv:2405.16712*, 2024. 1
- [10] Albert Gu and Tri Dao. Mamba: Linear-time sequence modeling with selective state spaces. *arXiv preprint arXiv:2312.00752*, 2023. 1, 2
- [11] Albert Gu, Karan Goel, and Christopher Ré. Efficiently modeling long sequences with structured state spaces. *arXiv preprint arXiv:2111.00396*, 2021. 1
- [12] Ali Hatamizadeh and Jan Kautz. Mambavision: A hybrid mamba-transformer vision backbone. *arXiv preprint arXiv:2407.08083*, 2024. 1, 6, 7
- [13] Kaiming He, Xiangyu Zhang, Shaoqing Ren, and Jian Sun. Deep residual learning for image recognition. In *Proceedings of the IEEE conference on computer vision and pattern recognition*, pages 770–778, 2016. 1, 2, 5, 6, 7
- [14] Kaiming He, Georgia Gkioxari, Piotr Dollár, and Ross Girshick. Mask r-cnn. In *Proceedings of the IEEE International Conference on Computer Vision (ICCV)*, pages 2961–2969, 2017. 6
- [15] Adamu Lawan, Juhua Pu, Haruna Yunusa, Aliyu Umar, and Muhammad Lawan. Enhancing long-range dependency with state space model and kolmogorov-arnold networks for aspect-based sentiment analysis. In *Proceedings of the 31st International Conference on Computational Linguistics*, pages 2176–2186, 2025. 1
- [16] Aobo Liang, Xingguo Jiang, Yan Sun, Xiaohou Shi, and Ke Li. Bi-mamba+: Bidirectional mamba for time series forecasting. *arXiv preprint arXiv:2404.15772*, 2024. 1
- [17] Opher Lieber, Barak Lenz, Hofit Bata, Gal Cohen, Jhonathan Osin, Itay Dalmedigos, Erez Safahi, et al. Jamba: A hybrid transformer-mamba language model. *arXiv preprint arXiv:2403.19887*, 2024. 1
- [18] Tsung-Yi Lin, Michael Maire, Serge Belongie, James Hays, Pietro Perona, Deva Ramanan, Piotr Dollár, and C. Lawrence Zitnick. Microsoft coco: Common objects in context. In *Computer Vision—ECCV 2014: 13th European Conference, Zurich, Switzerland, September 6-12, 2014, Proceedings, Part V*, pages 740–755. Springer International Publishing, 2014. 6
- [19] Yue Liu, Yunjie Tian, Yuzhong Zhao, Hongtian Yu, Lingxi Xie, Yaowei Wang, Qixiang Ye, Jianbin Jiao, and Yunfan Liu. Vmamba: Visual state space model. *Advances in neural information processing systems*, 37:103031–103063, 2025. 1, 3, 5, 6, 7
- [20] Ze Liu, Yutong Lin, Yue Cao, Han Hu, Yixuan Wei, Zheng Zhang, Stephen Lin, and Baining Guo. Swin transformer: Hierarchical vision transformer using shifted windows. In *Proceedings of the IEEE/CVF International Conference on Computer Vision*, pages 10012–10022, 2021. 6, 7
- [21] Zhuang Liu, Hanzi Mao, Chao-Yuan Wu, Christoph Feichtenhofer, Trevor Darrell, and Saining Xie. A convnet for the 2020s. In *Proceedings of the IEEE/CVF Conference on Computer Vision and Pattern Recognition*, pages 11976–11986, 2022. 5, 6, 7
- [22] Shusen Ma, Yu Kang, Peng Bai, and Yun-Bo Zhao. Fmamba: Mamba based on fast-attention for mul-

- tivariate time-series forecasting. *arXiv preprint arXiv:2407.14814*, 2024. 1
- [23] Xuezhe Ma, Xiang Kong, Sinong Wang, Chunting Zhou, Jonathan May, Hao Ma, and Luke Zettlemoyer. Luna: Linear unified nested attention. pages 2441–2453, 2021. 1, 2
- [24] Eric Nguyen, Karan Goel, Albert Gu, Gordon Downs, Preey Shah, Tri Dao, Stephen Baccus, and Christopher Ré. S4nd: Modeling images and videos as multidimensional signals with state spaces. In *Advances in Neural Information Processing Systems*, pages 2846–2861, 2022. 6
- [25] Badri N. Patro and Vijay S. Agneeswaran. Simba: Simplified mamba-based architecture for vision and multivariate time series. *arXiv preprint arXiv:2403.15360*, 2024. 1
- [26] Xiaohuan Pei, Tao Huang, and Chang Xu. Efficientv-mamba: Atrous selective scan for light weight visual mamba. *arXiv preprint arXiv:2403.09977*, 2024. 6
- [27] Ilija Radosavovic, Raj Prateek Kosaraju, Ross Girshick, Kaiming He, and Piotr Dollár. Designing network design spaces. In *Proceedings of the IEEE/CVF conference on computer vision and pattern recognition*, pages 10428–10436, 2020. 1, 6
- [28] Liliang Ren, Yang Liu, Yadong Lu, Yelong Shen, Chen Liang, and Weizhu Chen. Samba: Simple hybrid state space models for efficient unlimited context language modeling. *arXiv preprint arXiv:2406.07522*, 2024. 1, 2
- [29] Yair Schiff, Chia-Hsiang Kao, Aaron Gokaslan, Tri Dao, Albert Gu, and Volodymyr Kuleshov. Caduceus: Bi-directional equivariant long-range dna sequence modeling. *arXiv preprint arXiv:2403.03234*, 2024. 2
- [30] Jeong-geun Song. Ufo-vit: High performance linear vision transformer without softmax. *arXiv preprint arXiv:2109.14382*, 2021. 1, 2
- [31] Aravind Srinivas, Tsung-Yi Lin, Niki Parmar, Jonathon Shlens, Pieter Abbeel, and Ashish Vaswani. Bottleneck transformers for visual recognition. In *Proceedings of the IEEE/CVF Conference on Computer Vision and Pattern Recognition*, pages 16519–16529, 2021. 5, 6
- [32] Christian Szegedy, Wei Liu, Yangqing Jia, Pierre Sermanet, Scott Reed, Dragomir Anguelov, Dumitru Erhan, Vincent Vanhoucke, and Andrew Rabinovich. Going deeper with convolutions. In *Proceedings of the IEEE conference on computer vision and pattern recognition*, pages 1–9, 2015. 1
- [33] Mingxing Tan and Quoc Le. Efficientnet: Rethinking model scaling for convolutional neural networks. In *International conference on machine learning*, pages 6105–6114, 2019. 1, 6
- [34] Hugo Touvron, Matthieu Cord, Matthijs Douze, Francisco Massa, Alexandre Sablayrolles, and Hervé Jégou. Training data-efficient image transformers & distillation through attention. In *International Conference on Machine Learning*, pages 10347–10357. PMLR, 2021. 6, 7
- [35] Xiaolong Wang, Ross Girshick, Abhinav Gupta, and Kaiming He. Non-local neural networks. In *Proceedings of the IEEE conference on computer vision and pattern recognition*, pages 7794–7803, 2018. 1, 2
- [36] Gui-Song Xia, Jingwen Hu, Fan Hu, Baoguang Shi, Xiang Bai, Yanfei Zhong, Liangpei Zhang, and Xiaoqiang Lu. Aid: A benchmark data set for performance evaluation of aerial scene classification. *IEEE Transactions on Geoscience and Remote Sensing*, 55 (7):3965–3981, 2017. 7
- [37] Tete Xiao, Yingcheng Liu, Bolei Zhou, Yuning Jiang, and Jian Sun. Unified perceptual parsing for scene understanding. In *Proceedings of the European Conference on Computer Vision (ECCV)*, pages 418–434, 2018. 6
- [38] Xiong Xiao Xu, Canyu Chen, Yueqing Liang, Baixiang Huang, Guangji Bai, Liang Zhao, and Kai Shu. Sst: Multi-scale hybrid mamba-transformer experts for long-short range time series forecasting. *arXiv preprint arXiv:2404.14757*, 2024. 1
- [39] S. Yang, Y. Wang, and H. Chen. Mambamil: Enhancing long sequence modeling with sequence reordering in computational pathology. *arXiv preprint arXiv:2403.06800*, 2024. 2
- [40] Yuedong Yang, Hung-Yueh Chiang, Guihong Li, Diana Marculescu, and Radu Marculescu. Efficient low-rank backpropagation for vision transformer adaptation. 2024. 1, 2
- [41] Fisher Yu and Vladlen Koltun. Multi-scale context aggregation by dilated convolutions. In *Proceedings of the International Conference on Learning Representations (ICLR)*, 2016. 1, 2
- [42] Fisher Yu, Vladlen Koltun, and Thomas Funkhouser. Dilated residual networks. In *Proceedings of the IEEE conference on computer vision and pattern recognition*, pages 472–480, 2017. 1, 2
- [43] Haruna Yunusa, Shiyin Qin, Abdulrahman Hamman Adama Chukkol, Isah Bello, and Adamu Lawan. iianet: Inception inspired attention hybrid network for efficient long-range dependency. *arXiv preprint, arXiv:2407.07603*, 2024. 5
- [44] Bolei Zhou, Hang Zhao, Xavier Puig, Tete Xiao, Sanja Fidler, Adela Barriuso, and Antonio Torralba. Semantic understanding of scenes through the ade20k dataset. *International Journal of Computer Vision*, 127:302–321, 2019. 6

- [45] Lianghui Zhu, Bencheng Liao, Qian Zhang, Xinlong Wang, Wenyu Liu, and Xinggang Wang. Vision mamba: Efficient visual representation learning with bidirectional state space model. *arXiv*, 2024. [1](#), [3](#), [5](#), [6](#)